

---

# Simultaneous Phosphorescence and Fluorescence Lifetime Imaging by Multi-Dimensional TCSPC and Multi-Pulse Excitation

# 2

Wolfgang Becker, Vladislav Shcheslavskiy,  
and Angelika Rück

---

## Abstract

TCSPC FLIM/PLIM is based on a multi-dimensional time-correlated single-photon counting process. The sample is scanned by a high-frequency-pulsed laser beam which is additionally modulated on/off synchronously with the pixels of the scan. FLIM is obtained by building up the distribution of the photons over the scanning coordinates and the times of the photons in the excitation pulse sequence, PLIM is obtained by building up the photon distribution over the scanning coordinates and the photon times in the modulation period. FLIM and PLIM data are thus obtained simultaneously within the same imaging process. Since the technique uses not only one but many excitation pulses for every phosphorescence signal period the sensitivity is much higher than for techniques that excite with a single pulse only. TCSPC FLIM/PLIM works both with one-photon and two-photon excitation, does not require a reduction of the laser pulse repetition rate by a pulse picker, and eliminates the need of high pulse energy for phosphorescence excitation.

---

## Keywords

Fluorescence • Phosphorescence • FLIM • PLIM • TCSPC • Metabolic imaging • pO<sub>2</sub> imaging

---

## 2.1 Motivation of Using Phosphorescence Lifetime Imaging

Phosphorescence occurs when an excited molecule transits from the first excited singlet state, S<sub>1</sub>, into the first triplet state, T<sub>1</sub>, and returns

---

W. Becker (✉) • V. Shcheslavskiy • A. Rück  
Becker & Hickl GmbH, Berlin, Germany  
e-mail: [becker@becker-hickl.de](mailto:becker@becker-hickl.de)

from there to the ground state by emitting a photon [1]. Both the S1-T1 transition and the T1-S0 transition are ‘forbidden’ processes. The transition rates are therefore much smaller than for the S1-S0 transition. That means that phosphorescence is a slow process, with lifetimes on the order of microseconds or even milliseconds. Phosphorescence of organic dyes or endogenous fluorophores is extremely weak or even not detectable at room temperature. However, strong phosphorescence with lifetimes from the microsecond up to the millisecond range is obtained for lanthanide complexes [2] and organic complexes of ruthenium [1, 3], platinum [1, 4–6], terbium, and palladium [5]. Of special interest for live-cell imaging is that the phosphorescence of these complexes is strongly quenched by oxygen. The dyes are therefore excellent oxygen sensors [1, 5–10]. Applications are aiming at the measurement of oxygen partial pressure ( $pO_2$ ) in biological objects, and its effect on the metabolism of the cells. To reach this target it is desirable that PLIM and FLIM measurements are performed simultaneously. The oxygen concentration is then derived from the PLIM data, the metabolic information from the FLIM data, preferably from the NAD(P)H and the FAD fluorescence [11].

Metabolic imaging requires that the FLIM process resolves the bound and the unbound decay components of NAD(P)H and FAD, which requires an instrument response function shorter than 200 ps and a time-channel width of about 50 ps. The recording process must provide an optimum photon efficiency, i.e. a maximum signal-to-noise ratio of the recorded fluorescence and phosphorescence lifetimes for a given number of photons. Moreover, it is important that the imaging process delivers data from a defined plane inside cells or tissues, that it suppresses lateral and longitudinal scattering, and that it does so without compromising the photon efficiency. A strict requirement is compatibility with deep tissue imaging by multiphoton excitation and non-descanned detection. The only technique that meets these requirements is the combination of multi-dimensional TCSPC and laser scanning [12–15].

TCSPC FLIM has taken an impressive development in the last decade. Images as large as 2048 x 2048 pixels can be recorded without compromising the time resolution, and additional parameters can be included in the recording process [13, 16, 17]. As a result, TCSPC FLIM not only records conventional FLIM images at high resolution but also z stacks, lateral mosaics, multi-wavelength images, images at several excitation wavelengths, and images of fast dynamic effects induced in the sample. Moreover, TCSPC FLIM has been extended to record PLIM simultaneously with FLIM [13, 18]. Challenges, solutions, and typical applications of combined FLIM/PLIM will be described in this chapter.

---

## 2.2 Technical Challenges

### 2.2.1 Excitation Pulse Period and Laser Power

The obvious problem of PLIM is that the excitation pulse period must be a few times longer than the phosphorescence decay time. For ruthenium dyes with phosphorescence lifetimes below 1  $\mu$ s the reduction in laser repetition rate may still be feasible, see Hosny et al. [3]. However, the lifetimes for platinum and palladium-based dyes are on the order of 50–100  $\mu$ s, and the lifetimes of europium and terbium dyes can be in the millisecond range. PLIM with these dyes would require a laser repetition rate of less than 10 kHz. Reducing the repetition rate—if possible at all—results in a substantial decrease in the average excitation power, and, consequently, decrease in phosphorescence intensity, see Fig. 2.1a. Attempts to compensate for the decrease in average power by higher peak power are limited by the capabilities of the laser, by saturation and other nonlinear effects in the sample, or, in multiphoton systems, unwanted excitation of higher energy levels or even ionisation. In other words, the effect of reducing the excitation pulse rate is poor sensitivity. Low sensitivity can partially be compensated by high concentration of the phosphorescence marker.

However, the commonly used phosphorescence dyes are potentially toxic, and using them in high concentration is not desirable.

### 2.2.2 Pile-Up Effect

Simply reducing the laser repetition rate causes a significant problem for recording FLIM simultaneously with PLIM. In principle, it would be possible to derive FLIM and PLIM data from a one and the same decay curve that is excited by low-repetition rate laser pulses and simultaneously recorded at two different time scales. One channel would record a photon distribution over the FLIM time scale, the other over the PLIM time scale. However, this would unavoidably create a pile-up problem for the FLIM channel. The lifetimes of the decay components are in the range from a few 100 ps to a few nanoseconds. Neither the detector nor the TCSPC electronics of the FLIM channel are able to detect several photons within this time and determine their arrival times at picosecond accuracy. Detection of several photons per excitation pulse must therefore be avoided. That means the detection rate must be kept at a level no higher than 10% of the excitation rate [12–14]. This is not a problem for FLIM with laser repetition rates in the 50–80 MHz range. However, for excitation rates on the order of 100 kHz (for Ruthenium) and 10 kHz (for Platinum and Palladium) the available detection rates would become extremely low, and, consequently, the acquisition times unacceptably long.

### 2.2.3 Detector Overload

Another problem is that any sample that emits phosphorescence necessarily also emits fluorescence. The fluorescence both comes from endogenous fluorophores of the sample, and from singlet emission of the phosphorescence probe. At high laser peak power the peak power of fluorescence becomes extremely high, see Fig. 2.1b. This causes transient overload and extreme after-pulsing in the detectors. It is then impossible to detect a correct phosphorescence decay in the

first few microseconds after the laser pulse. In principle, the overload problem can be solved by using laser pulses with a duration in the microsecond range. However, apart from the fact this is not simply feasible with most lasers it would make simultaneous FLIM impossible. Moreover, microsecond pulse duration is not an option for multiphoton excitation.

### 2.2.4 Interference with Scanning

PLIM in scanning systems has also another problem. The time the scanner stays within the excited sample volume must be longer than the phosphorescence lifetime. If the scanner runs off the excited volume within the phosphorescence decay time photons in the tail of the decay function are lost, and the recorded decay profile gets distorted, see Fig. 2.1c. Reasonable recording, even of pure intensity images, can thus be obtained only by sufficiently slow scanning. Moreover, the pixel time and the excitation pulse period are on the same order of magnitude. The number of excitation pulses in the individual pixels can thus vary systematically and induce Moiré effects in the images, see Fig. 2.1d. The problem can be solved by synchronising the laser pulses with the pixel frequency, but there is usually no provision for this in normal laser scanning microscopes. Without synchronisation, the pixel time had to be at least 100 times longer than the laser period. This leads to extremely long scan times, and to a further increase of the acquisition time (Fig. 2.1).

## 2.3 FLIM—PLIM by Multipulse Excitation

The problems described above are avoided by a FLIM/PLIM technique developed by bh in 2010 [18]. The technique is based on the idea that, if a single short laser pulse is not efficient in exciting phosphorescence, a burst of multiple laser pulses will perform much better. As long as the burst duration is shorter than the phosphorescence lifetime the excitation efficiency will increase in proportion to the number of pulses within the burst.

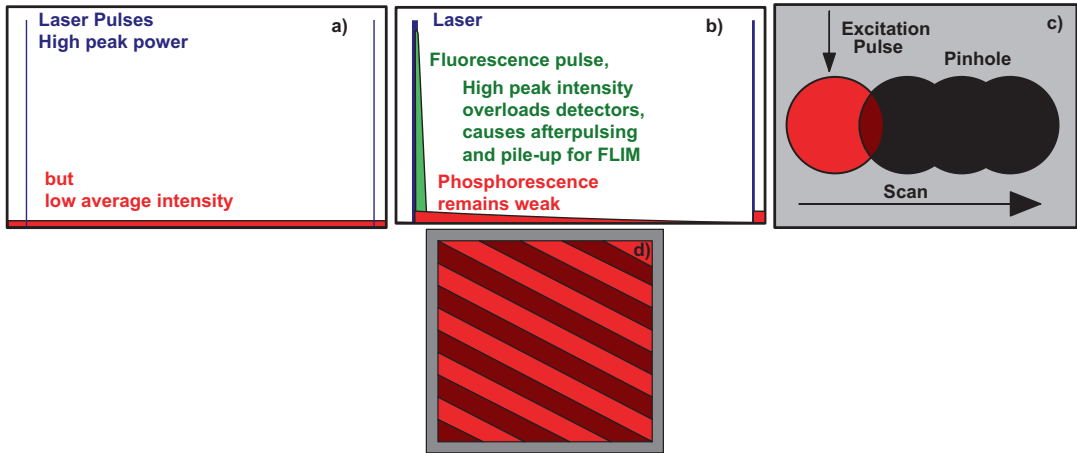


**Fig. 2.1** Challenges of PLIM. (a) Low laser repetition rate results in low average excitation intensity. (b) High peak-to-average power ratio causes high peak intensity of fluorescence, detector overload and afterpulsing, and pile-up in parallel FLIM recording. The phosphorescence

intensity remains low due to low average excitation power. (c) Scanning must be slow enough to stay in the excited pixel over the time of the phosphorescence decay. (d) Low scan rate interferes with low laser pulse repetition rate. This induces Moiré effects in the images

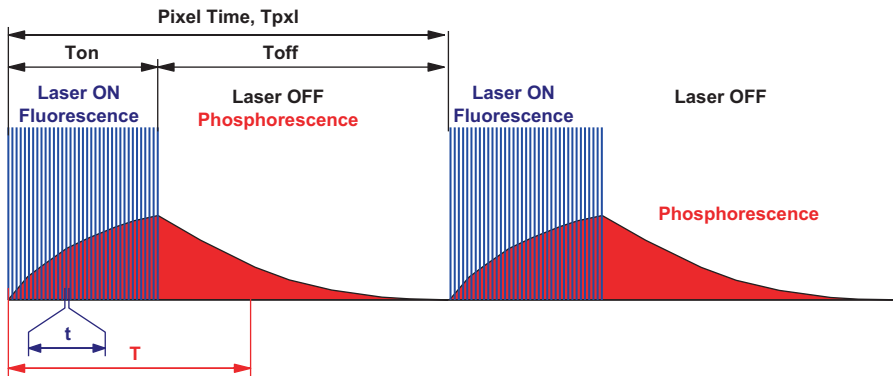


**Fig. 2.2** Principle of Microsecond FLIM. A high-frequency pulsed laser is on-off modulated synchronously with the pixels. FLIM is recorded in the Laser ON phases, PLIM in the Laser OFF phases

Multi-pulse excitation has been used for multi-photon phosphorescence imaging earlier [6] but bh were first to apply it to TCSPC PLIM.

The principle is shown in Fig. 2.2. The sample is excited by a pulsed laser running at a repetition rate in the 50–80 MHz range, i.e. at a repetition rate as it is typically used for TCSPC FLIM. However, the laser does not run continuously. Instead, it is turned on only for a given period of time,  $T_{on}$ , at the beginning of each pixel. Within the on-time,  $T_{on}$ , the laser pulses excite

fluorescence, and, pulse by pulse, build up phosphorescence. The phosphorescence intensity at the end of the laser-on time is far higher than for a single laser pulse.

For the rest of the pixel time the laser is turned off. After the last laser pulse, the fluorescence decays quickly, and for the rest of the pixel dwell time,  $T_{off}$ , pure phosphorescence is detected.

The build-up of TCSPC FLIM and PLIM images with this excitation sequence is straightforward. For each photon, the TCSPC module

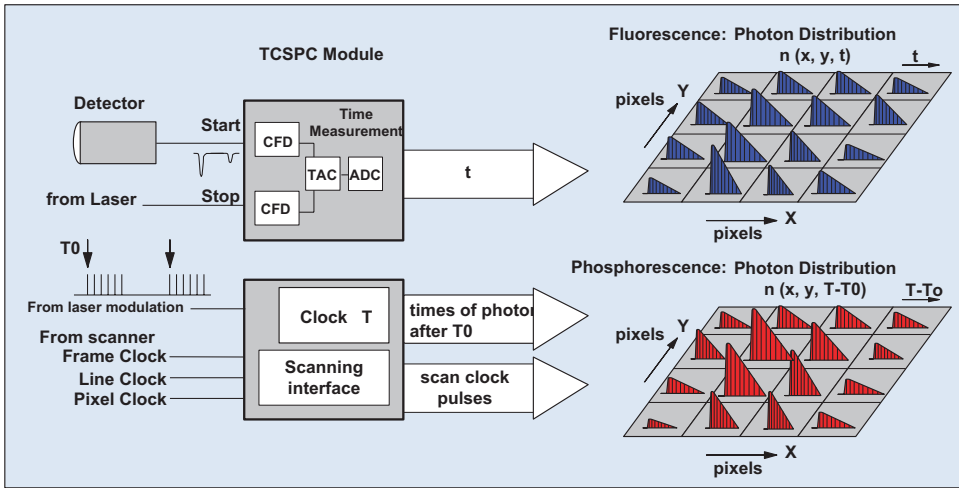


**Fig. 2.3** Simultaneous fluorescence and phosphorescence lifetime imaging

determines the time,  $t$ , within the laser pulse period, and the time,  $T$ , after the start of the modulation pulse. The TCSPC process builds up photon distributions over these times and the scan coordinates [14, 16, 18–20].

The TCSPC principle is shown in Fig. 2.3. A fluorescence lifetime image is obtained by building up a photon distribution over the times,  $t$ , of the photons in the laser pulse period, and the scanner position,  $x, y$ , during the  $T_{on}$  periods. The phosphorescence lifetime image is obtained by building up a similar distribution over the times,  $T$ , within the laser modulation period and the beam position,  $x, y$ . Thus, fluorescence and phosphorescence lifetime images are obtained simultaneously, in the same scan, and from photons excited by the same laser pulses.

The procedure can be further refined by using the laser on/off information as a routing signal to better separate the fluorescence in laser-on phases from the phosphorescence in the laser-off phases, please see [13, 21, 22] for details.

The principle solves all the problems discussed in the previous section. The excitation pulse rate of FLIM gets de-coupled from the excitation rate of PLIM: The FLIM excitation rate is the laser pulse period, the PLIM excitation period is the period of the on/off modulation. The average excitation intensity drops only by the duty cycle of the laser modulation, and the effec-

tive FLIM excitation rate remains high. High phosphorescence intensity is obtained, and there is no problem with pile-up. The peak intensity of the laser pulses need not be higher than for a normal TCSPC FLIM measurement. The principle thus remains compatible with multiphoton excitation. Moreover, there is no excessively high fluorescence peak intensity, and no detector overload problem. Also the Moiré problem is solved: The laser modulation is automatically synchronised with the pixels of the scan. Every pixel thus gets the same number of excitation pulses.

## 2.4 Implementation in Laser Scanning Systems

The implementation of combined FLIM/PLIM in a laser scanning microscope requires that the microscope has or can be upgraded with a pulsed excitation laser, and that this laser can be on/off modulated by a signal from the scanner or from the FLIM/PLIM electronics. Picosecond diode lasers can be modulated electronically, supercontinuum Lasers can be modulated via the AOTF (acousto-optical filter) that is normally used to select the desired wavelength. In multiphoton microscopes the Ti:Sapphire lasers can normally be modulated via the AOM or EOM that is used to control the intensity.

Moreover, it must be possible to select a sufficiently slow scan speed that avoids that the scanner is running off the excited pixel during the phosphorescence decay time. The required pixel times up to about 100  $\mu\text{s}$  are available in almost any laser scanning microscope.

### 2.4.1 DCS-120 Confocal Scanning FLIM System

Laser on/off modulation in the bh DCS-120 laser scanning system [21] is integrated in the scan controller hardware. The modulation is achieved via the laser multiplexing function of the scan controller module. The DCS system normally has two lasers which can be multiplexed within one pixel. PLIM operation for one laser is obtained by enabling the pixel multiplexing function, and turning the second laser off. The laser then turns on at the beginning of each pixel, runs for a fraction of the pixel time, and then turns off. The multiplexing function also routes photons from the 'Laser ON' and 'Laser OFF' phases into different memory blocks, and thus provides separate images for the FLIM and PLIM signal, and the total luminescence. The laser on/off function is the same for systems with diode lasers, with a supercontinuum laser, and for multiphoton systems with a Ti:Sapphire laser. Different than other laser scanning systems, the DCS-120 scanner has an option to run along the lines in steps of the individual pixels. This avoids that the scanner runs off the excited spot during the pixel time.

### 2.4.2 Zeiss LSM 710, 780, 880 Systems

For the FLIM systems for the Zeiss LSM 710 /780/880 microscope family [21] a bh DDG-210 pulse generator card is added to the FLIM system. The DDG card triggers on the pixel clock of the LSM, and sends a 'Laser On' signal to the laser controller of the microscope. The principle is shown in Fig. 2.4. The pixel clock is split off from the scan synchronisation cable and connected into the trigger input of the DDG card. The 'Laser On' signal is connected into the laser control module of the Zeiss LSM via a 'PLIM' input. This input is optional; it has to be ordered from Zeiss via an 'INDIMO' (individual modification) request. PLIM Laser control via the DDG-210 card is integrated in the bh SPCM software. The card also generates a 'routing' signal that directs the photons from the 'Laser ON' phases and the 'Laser OFF' phases into different memory blocks of the TCSPC system. This way, separate images for the FLIM signal, the PLIM signal, and the total luminescence signal can be provided and displayed during the measurement. Please see [21] for further details.

### 2.4.3 Leica SP Multiphoton Systems

As for the Zeiss LSMs, the laser on-off function is controlled by a bh DDG-210 pulse generator module that is added to the FLIM system. The card is triggered by the pixel clock of the microscope. The on-off signal from the DDG is fed

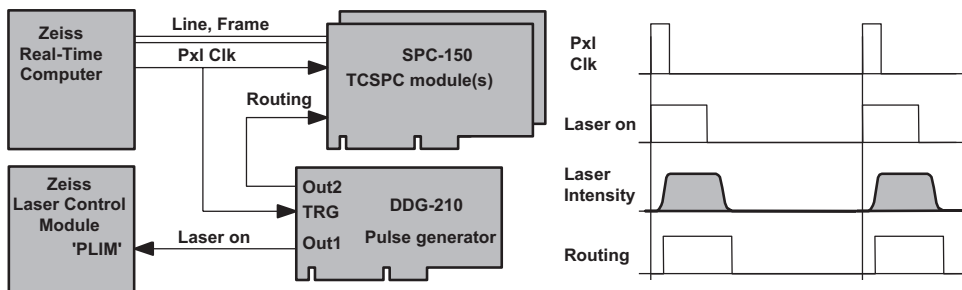


**Fig. 2.4** Left: Principle of laser on/off control for the Zeiss LSMs

into the beam blanking control of the microscope via a logic gate.

Laser power control in the Leica multiphoton systems is performed by an EOM (electro-optical modulator). The EOM is fast enough for PLIM on-off modulation. However, we often found that it does not turn the laser entirely off, especially when the EOM control parameters are not accurately adjusted. This is no problem in standard imaging applications but it can be a problem for PLIM. Spurious excitation during the 'laser-off' phases causes a large background in the phosphorescence decay or even makes it impossible to record phosphorescence at all. The solution is an ND filter in the excitation beam path. FLIM/PLIM is performed at no more than 5% of the available laser power. A filter that transmits about 20% shifts the power range from 0–5% to 0–25%, and reduces the laser power in the off phases sufficiently to avoid spurious excitation. A reflective filter should be used (an absorptive filter may crack).

The Leica systems use a sinusoidal scan in x direction. The nonlinearity of the scan is compensated by a non-uniform pixel time. This is not a problem for the bh FLIM systems: The bh systems use the pixel clock from the Leica scanner and thus avoid distortion of the images [15]. For PLIM, however, the variable pixel time results in a variable laser on/off period along the lines and a variable effective PLIM excitation rate. Also this is not normally a problem. However, the scan rate should be selected slow enough to let the phosphorescence completely decay within the pixel time. Normally, incomplete decay can be taken into account by a suitable model in the SPCImage data analysis [13]. However, this requires that the excitation period is constant over the entire image. This is not the case for PLIM with the Leica microscopes.

#### 2.4.4 Sutter Instrument MOM Microscopes

The Sutter Instrument MOM (movable objective) microscope [22] is a modular platform for imaging deep within live samples. It uses multi-photon

excitation by a titanium-sapphire laser in combination with non-descanned detection. Typical applications of the MOM system are autofluorescence imaging of cells, and autofluorescence imaging in tissue and whole organisms. These benefit considerably from the combination with FLIM/PLIM. The general principle is the same as for the Zeiss and Leica multiphoton microscopes. The difference is that there is no direct input for a laser on/off signal. Instead, the intensity-control signal of the Sutter system is coupled out via an existing connector and multiplied with the laser ON/OFF modulation signal from a DDG-210 card. The combined signal is fed back into the intensity-control signal path of the MOM system.

## 2.5 Applications

### 2.5.1 Oxygen Sensing

Oxygen sensing by PLIM has become a hot topic in biomedical microscopy, see [5–10]. Until recently, phosphorescence imaging has mainly been performed by gated camera techniques. The disadvantage of the camera is that does not suppress out-of-focus light and lateral and longitudinal scatterin. A camera is therefore not a good solution for deep-tissue imaging. PLIM by the technique described here solves these problems by confocal and two-photon laser scanning microscopy, and, additionally, yields FLIM and PLIM simultaneously. An increasing number of publications therefore aims at the use of PLIM for oxygen sensing in cells and tissue. Toncelly et al. used the technique to characterize the sensor dyes [23]. The penetration into cells and the behaviour of the dyes in the biological environment was investigated by Dmitriev et al. [24]. The response of the cells and cell clusters to variation in the oxygen concentration under physiological conditions has been investigated by [9, 25–28]. Lukina et al. used single-point fluorescence/phosphorescence decay measurements to measure the metabolic activity and the oxygen concentration in tumors in live mice via a fibre-optical system [29]. An overview on the FLIM/



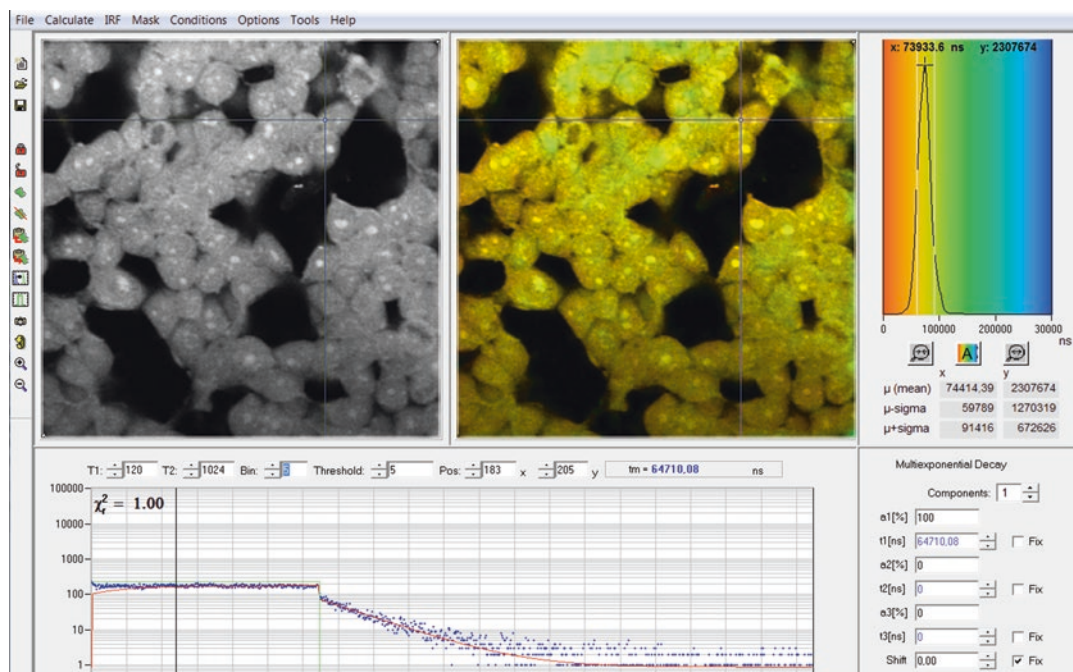


**Fig. 2.5** HEK cells incubated with a palladium dye under atmospheric oxygen partial pressure. Recorded by bh DCS-120 confocal scanning system, data analysis by bh SPCImage. Lifetime scale 0 (red) to 300  $\mu$ s (blue).

Phosphorescence lifetime at the Cursor-Position 65  $\mu$ s. The maximum of the lifetime distribution over the pixels is at 75  $\mu$ s

PLIM technique and an introduction into the use of an oxygen-sensitive solid matrix for cells has been given by Jenkins et al. [30].

Examples are shown in the figures below. Figures 2.5 and 2.6 show cultured human embryonic kidney cells incubated with a palladium-based phosphorescence dye. Figure 2.5 was recorded under atmospheric oxygen partial pressure. The maximum of the lifetime distribution over the pixels is at 75  $\mu$ s. Figure 2.6 was recorded under decreased oxygen partial pressure. As expected, the maximum of the lifetime distribution has shifted to longer decay times, in this case 144  $\mu$ s.

### 2.5.2 Simultaneous Recording of $pO_2$ and NAD(P)H Images

Simultaneously recorded fluorescence and phosphorescence lifetime images of live cultured human squamous carcinoma (SCC-4) cells stained with tris (2,2'-bipyridyl) dichlororuthen-

nium (II) hexahydrate are shown in Fig. 2.7, left and right. The data were acquired by a Zeiss LSM 780 NLO multiphoton microscope with a bh Simple-Tau 152 TCSPC system. The excitation wavelength was 750 nm. The image on the left was recorded in a wavelength interval from 440 to 480 nm. It contains mainly fluorescence of NAD(P)H. The data were analysed with a double-exponential decay model. The image shows the ratio of the amplitudes,  $a_1$  and  $a_2$ , of the decay components. The  $a_1/a_2$  ratio directly represents the ratio of unbound ( $a_1$ ) and bound ( $a_2$ ) NAD(P)H. The image on the right is the PLIM image. It shows the phosphorescence lifetime of the Ruthenium dye. The lifetime is reciprocally related to the oxygen concentration.

Although the results obtained so far look promising caution appears indicated when PLIM data are interpreted in terms of absolute  $O_2$  concentration measurement. As can be seen from Fig. 2.7 the ruthenium dye binds to the constituents of the cells. The phosphorescence



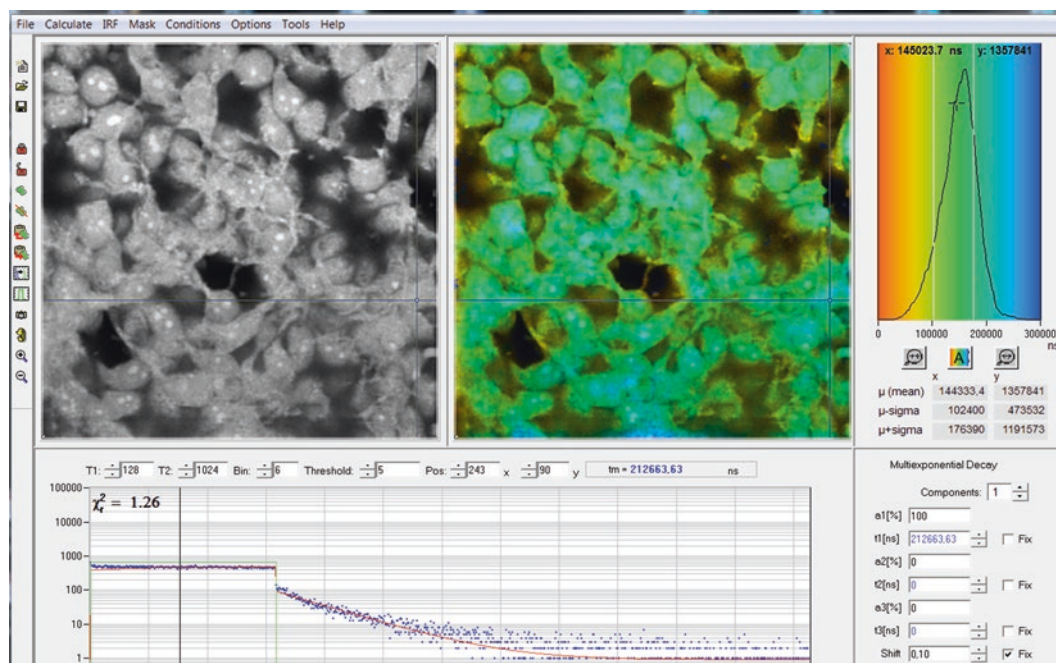
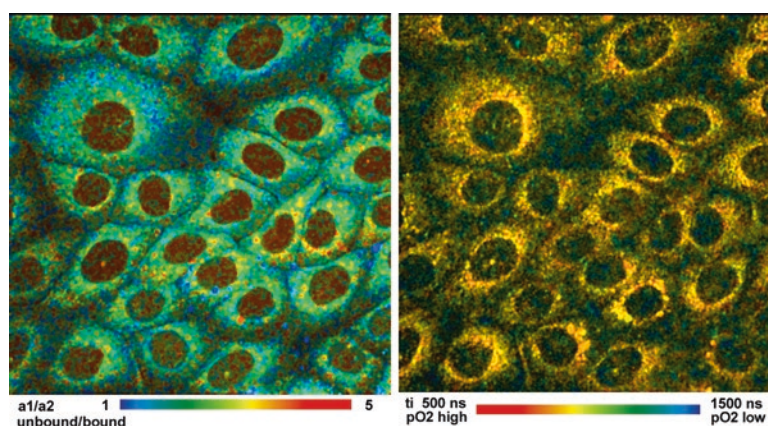


**Fig. 2.6** HEK cells incubated with a palladium dye under reduced oxygen partial pressure. Recorded by bh DCS-120 confocal scanning system, data analysis by bh SPCImage. Lifetime scale 0 (red) to 300  $\mu$ s (blue).

Phosphorescence lifetime at the Cursor-Position 212  $\mu$ s. The maximum of the lifetime distribution over the pixels is at 144  $\mu$ s

**Fig. 2.7** FLIM and PLIM images of SCC-4 cells stained with (2,2'-bipyridyl) dichlororuthenium (II) hexahydrate. FLIM shown *left*, PLIM shown *right*. Zeiss LSM 780 NLO with PLIM option, bh Simple-Tau 152 FLIM/PLIM system, 2-photon excitation at 750 nm



lifetime of bound and unbound dye can be different. Moreover, quenching phenomena are at least in part diffusion-controlled. The quenching rate - and thus the sensitivity to oxygen - more or less depends on the oxygen diffusion constant. The

diffusion constant may be different inside the cells and outside, and in different compartments of the cells.  $pO_2$  results derived from PLIM decay times may therefore not necessarily be comparable for different sub-structures of the cells.

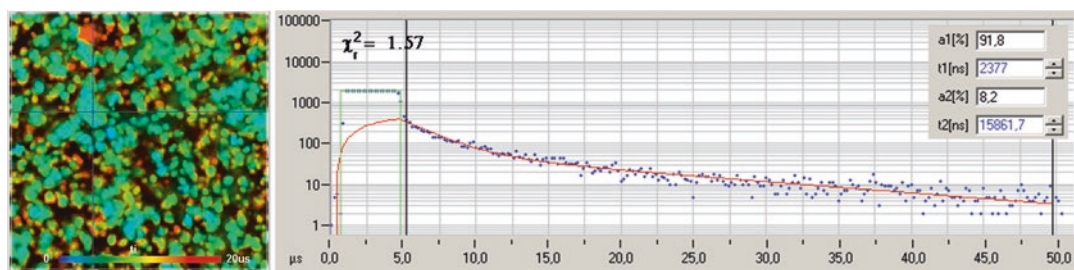


**Fig. 2.8** PLIM of zinc oxide nanoparticles. *Left:* Lifetime image, intensity weighted lifetime of double-exponential fit. *Right:* Decay curve at cursor position. Zeiss LSM 710, two-photon excitation at 750 nm, non-descanned detection

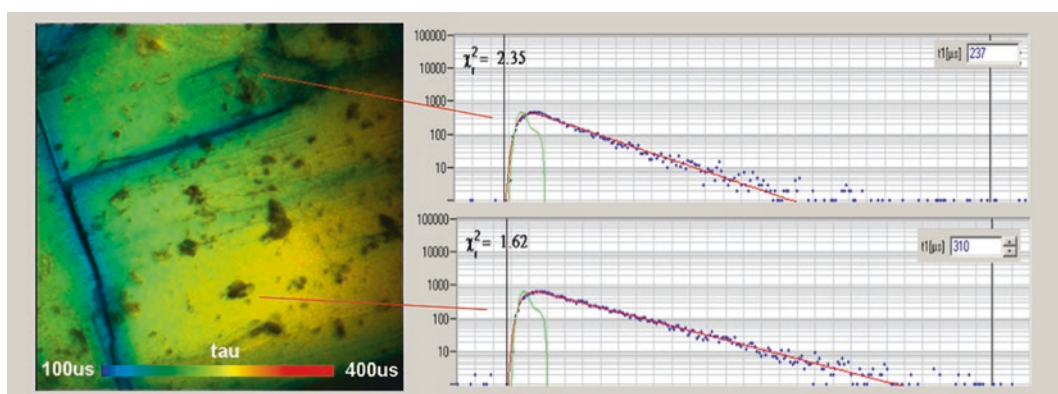


**Fig. 2.9** PLIM image of a uranium mineral. Decay curves if two arbitrary selected spots are shown on the right. 256 × 256 pixels, 256 time channels, pixel time 3.6 ms, excitation 405 nm, emission filter long pass 435 nm

### 2.5.3 Detection of Zinc Oxide Nanoparticles

Nanoparticles often emit luminescence with decay times in the microsecond range. This makes them distinguishable from biological tissue which normally does not emit any detectable amount of phosphorescence. PLIM signals can thus be used to identify nanoparticles in biological tissue, and follow their migration or possible dissolution. The principle has been used to track ZnO nanoparticles from sunscreens or cosmetic products in human skin, and investigate possible influence on the viability by simultaneously recording the fluorescence of NAD(P)H [31]. Figure 2.8 shows zinc oxide particles detected by PLIM. The decay function is multi-exponential, with average (intensity-weighted) lifetimes up to 20  $\mu$ s.

### 2.5.4 PLIM of Inorganic Materials

Figure 2.9 was obtained from an Autumit crystal (a uranium mineral). The phosphorescence lifetimes vary from about 100–400  $\mu$ s. The lifetime image is shown on the left, decay curves of two selected spots on the right. The pixel time was 3.6 ms, the laser-on time 200  $\mu$ s. The excitation wavelength was 405 nm, a 435 nm long pass filter was used in the emission path.

## 2.6 Suppression of Autofluorescence

Other applications are using PLIM for the suppression of autofluorescence. The sample is stained with a phosphorescent dye, and the long lifetime is used as a discrimination param-

eter [32, 33]. The SPCM software of the bh FLIM/PLIM systems offers this option online, without the need of special data analysis, see [13, 21].

## 2.7 Summary

Compared with PLIM techniques that use a single excitation pulse for every phosphorescence decay cycle the techniques described here has a number of significant advantages. The first one is that excitation with multiple pulses obtains a significantly higher triplet population than excitation with a single pulse. The sensitivity is therefore much higher. The technique can thus be used at correspondingly lower concentration of the phosphorescence probe, which, in turn, helps reduce possible toxicity. The second advantage is that it is compatible with multiphoton excitation. Due to the excitation with multiple laser pulses it does not require higher laser power or laser pulse energy than normal confocal or multiphoton FLIM. A third advantage is related to the TCSPC technique itself. TCSPC FLIM can record no more than one photon per laser pulse. The photon rate thus has to be limited to no more than 10% of the excitation pulse rate. This is no problem for the 80 MHz or 50 MHz pulse rates of Ti:Sapphire or picosecond diode lasers but it would be a problem if the pulse repetition rate was reduced to the kHz range. The technique described avoids this limitation because it works at the full laser repetition rate. The acquisition times is therefore on the order of 10–100 s, depending on the expectations to the signal-to-noise ratio of the lifetimes [12, 13]. The only remaining limitation is in the scan rate. The pixel time must not be shorter than about five times the phosphorescence decay time. This leads to minimum frame times in the range of 1 s for ruthenium dyes and about 10 s for platinum dyes. This no longer than the acquisition time required to obtain the desired signal-to-noise ratio. It thus has no influence on the total acquisition time of the FLIM/PLIM process.

## References

1. Lakowicz JR (2006) Principles of fluorescence spectroscopy, 3rd edn. Springer, Heidelberg
2. Charbonniere LJ, Hildebrandt N (2008) Lanthanide complexes and quantum dots: a bright wedding for resonance energy transfer. *Eur J Inorg Chem* 2008:3241–3251
3. Hosny NA, Lee DA, Knight MM (2012) Single photon counting fluorescence lifetime detection of pericellular oxygen concentrations. *J Biomed Opt* 17(1):016007-1–016007-12
4. Fercher A, Borisov SM, Zhdanov AV et al (2011) Intracellular O<sub>2</sub> sensing probe based on cell-penetrating phosphorescent nanoparticles. *ACS Nano* 5:5499–5508
5. Lebedev AY, Cheprakov AV, Sakadzic S et al (2009) Dendritic phosphorescent probes for oxygen imaging in biological systems. *Appl Mater Interfaces* 1:1292–1304
6. Sakadžic S, Roussakis E, Yaseen MA et al (2010) Two-photon high-resolution measurement of partial pressure of oxygen in cerebral vasculature and tissue. *Nat Methods* 7:755–759
7. Gerritsen HC, Sanders R, Draaijer A et al (1997) Fluorescence lifetime imaging of oxygen in cells. *J Fluoresc* 7:11–16
8. Papkovsky D, Zhdanov AV, Fercher A et al (2012) Phosphorescent oxygen-sensitive probes. Springer
9. Papkovsky DB, Dmitriev RI (2013) Biological detection by optical oxygen sensing. *Chem Soc Rev* 42:8700–8732
10. Shibata M, Ichioka S, Ando J, Kamiya A (2001) Microvascular and interstitial PO<sub>2</sub> measurement in rat skeletal muscle by phosphorescence quenching. *J Appl Physiol* 91:321–327
11. Skala MC, Riching KM, Bird DK et al (2007) In vivo multiphoton fluorescence lifetime imaging of protein-bound and free nicotinamide adenine dinucleotide in normal and precancerous epithelia. *J Biomed Opt* 12:02401-1–02401-10
12. Becker W (2005) Advanced time-correlated single-photon counting techniques. Springer, Berlin, Heidelberg, New York
13. Becker W (2015) The bh TCSPC handbook, 6th edn. Becker & Hickl GmbH, Berlin. Available from: [www.becker-hickl.com](http://www.becker-hickl.com)
14. Becker W (2015) Introduction to multi-dimensional TCSPC. In: Becker W (ed) Advanced time-correlated single photon counting applications. Springer, Berlin, Heidelberg, New York, pp 1–63
15. Becker W, Shcheslavskiy V, Studier H (2015) TCSPC FLIM with different optical scanning techniques. In: Becker W (ed) Advanced time-correlated single photon counting applications. Springer, Berlin, Heidelberg, New York, pp 65–117
16. Becker W (2015) Fluorescence lifetime imaging by multi-dimensional time correlated single photon counting. *Med Photon* 27:41–61

17. Studier H, Becker W (2014) Megapixel FLIM. *Proc SPIE* 8948:89481K
18. Becker W, Su B, Bergmann A et al (2011) Simultaneous fluorescence and phosphorescence lifetime imaging. *Proc SPIE* 7903:790320
19. Becker W (2015) Fluorescence lifetime imaging techniques: time-correlated single-photon counting. In: Marcu L, French PMW, Elson DS (eds) *Fluorescence lifetime spectroscopy and imaging. Principles and applications in biomedical diagnostics*. CRC Press, Taylor & Francis Group, Boca Raton, London, New York, pp 203–232
20. Shcheslavskiy VI, Neubauer A, Bukowiecki R et al (2016) Combined fluorescence and phosphorescence lifetime imaging. *Appl Phys Lett* 108:091111-1–091111-5
21. Becker & Hickl GmbH (2015) DCS-120 confocal scanning FLIM systems. In: *User handbook*, 6th edn. Available from: [www.becker-hickl.com](http://www.becker-hickl.com)
22. Sutter instrument, Movable objective microscope. [www.sutter.com/microscopes](http://www.sutter.com/microscopes)
23. Toncelli C, Arzhakova OV, Dolgova A et al (2014) Oxygen-sensitive phosphorescent nanomaterials produced from high density polyethylene films by local solvent-crazing. *Anal Chem* 86(3):1917–1923
24. Dmitriev RI, Kondrashina AV, Koren K et al (2014) Small molecule phosphorescent probes for O<sub>2</sub> imaging in 3D tissue models. *Biomater Sci* 2:853–866
25. Dmitriev RI, Zhdanov AV, Nolan YM, Papkovsky DB (2013) Imaging of neurosphere oxygenation with phosphorescent probes. *Biomaterials* 34:9307–9317
26. Kalinina S, Shcheslavskiy V, Becker W et al (2016) Correlative NAD(P)H-FLIM and oxygen sensing-PLIM for metabolic mapping. *J Biophotonics* 9(8):800–811
27. Kurokawa H, Ito H, Inoue M et al (2015) High resolution imaging of intracellular oxygen concentration by phosphorescence lifetime. *Sci Rep* 5:1–13
28. Zhdanov AV, Golubeva AV, Okkelman IA et al (2015) Imaging of oxygen gradients in giant umbrella cells: an ex vivo PLIM study. *Am J Phys Cell Phys* 309:C501–C509
29. Lukina M, Orlova A, Shirmanova M et al (2017) Interrogation of metabolic and oxygen states of tumors with fiber-based luminescence lifetime spectroscopy. *Opt Lett* 42(4):731–734
30. Jenkins J, Dmitriev RI, Papkovsky DB (2015) Imaging cell and tissue O<sub>2</sub> by TCSPC-PLIM. In: Becker W (ed) *Advanced time-correlated single photon counting applications*. Springer, Berlin, Heidelberg, New York, pp 225–247
31. Sanchez WY, Pastore M, Haridass I et al (2015) Fluorescence lifetime imaging of the skin. In: Becker W (ed) *Advanced time-correlated single photon counting applications*. Springer, Berlin, Heidelberg, New York, pp 457–508
32. Baggaley E, Botchway SW, Haycock JW et al (2014) Long-lived metal complexes open up microsecond lifetime imaging microscopy under multiphoton excitation: from FLIM to PLIM and beyond. *Chem Sci* 5:879–886
33. Baggaley E, Gill MR, Green NH et al (2014) Dinuclear ruthenium(II) complexes as two-photon, time-resolved emission microscopy probes for cellular DNA. *Angew Chem Int Ed Eng* 53:3367–3371



Multi-Parametric Live Cell Microscopy of 3D Tissue  
Models

Dmitriev, R.I. (Ed.)

2017, XII, 172 p. 53 illus., 39 illus. in color., Hardcover

ISBN: 978-3-319-67357-8